ISSN: 2472-3703 DOI: 10.6911/WSRJ.202007_6(7).0038

Numerical Study on Two-Phase Heat Transfer and Flow of Subcooled Flow Boiling of R290 in A Vertical Tube

Dengchen Qi[1, a], Jiakai Zhang[1, b] and Wenzhong Gao[1, c, *]

[1]Merchant Marine College, Shanghai Maritime University, Shanghai, China.

[a]qidengchen@163.com, [b]zhangjiakai2020@163.com, [c]wzgao@shmtu.edu.cn

Abstract

This study numerically investigates the two-phase heat transfer and flow of R290 during subcooled flow boiling in a vertical tube. The operation condition of the simulations is as follows: 500kg/m²s for mass flux and 12kW/m² for heat flux. The simulations are carried out for 3D model using Fluent. The computations are based on two-fluid model combined with RPI wall boiling model. Main characteristics of subcooled flow boiling are analyzed, including vapor volume fraction, wall and bulk temperature, vapor and liquid velocity and heat transfer coefficient. The results show that heat transfer coefficient and wall temperature change significantly from single phase connective region to subcooled nuclear boiling region. The distributions of vapor volume fraction are different along axial and radial directions. There is a nearly constant trend for the rise of bulk temperature. Vapor velocity is lower than liquid velocity initially while exceed that finally.

Keywords

Subcooled flow boiling; two-phase flow; heat transfer; CFD.

1. INTRODUCTION

Subcooled flow boiling occurs in many technical applications such as steam generators, nuclear reactors and refrigeration systems. Similar to any boiling process, subcooled flow boiling is a phase change process where exists thermodynamic non-equilibrium between the liquid and vapor phases. Thus, the complexity of the process is increased and the analysis is very challenging.

There have been many studies on heat transfer and flow of flow boiling for R290 in recent decades. Choi et al. experimentally investigated the two-phase flow boiling pressure drop and heat transfer for R290 in horizontal minichannels with inner diameters of 1.5mm and 3.0mm. The experiment results showed that the pressure drop is higher for the conditions of higher mass and heat fluxes. Lillo et al. experimentally studied two-phase flow boiling heat transfer coefficient, pressure drop and dry-out incipience vapor quality data for R290 in a circular channel of a 6.0mm inner diameter. The results showed that at high mass fluxes and low heat fluxes, an increase of the saturation temperature leaded to higher heat transfer performances only for low vapor qualities. Despite the numerous studies on saturation flow boiling for R290, limited amount of data on subcooled flow boiling heat transfer and flow are available in literature, especially at low saturation temperatures.

With the rapid development of computer technology and computational fluid dynamics (CFD), multidimensional theoretical description and analysis of subcooled boiling flow have being performed. Among these, the most widely used and effective approach so far appears to be two-fluid model. Chen et al. used two-fluid model to simulate upward subcooled boiling flow

ISSN: 2472-3703 DOI: 10.6911/WSRJ.202007_6(7).0038

of R113. Their results showed good approximation with the experimental data. Gao et al. used two-fluid model to investigate the onset of significant void during water subcooled flow boiling. Good consistency between simulation results and available experimental data was obtained.

The aim of this study is to numerically investigate two-phase heat transfer and flow in subcooled flow boiling of R290 at low saturation temperature under a low mass flux and heat flux operation condition. Firstly, a 3D physical model is established to model a 1.56m long tube with an inner diameter of 6.0mm. Meanwhile, a mathematical model is proposed, based on two-fluid model, k-e turbulence model and RPI wall boiling model. Then, the accuracy of numerical results is evaluated compared to an experimental correlation. Finally, characteristics of void fraction, wall and bulk temperature, vapor and liquid velocity and heat transfer coefficient are discussed.

2. NUMERICAL SCHEMES

2.1. Two-fluid Model

For this work, the liquid phase is considered a continuous phase, and the vapor is treated as a dispersed phase. The governing equations of two-phase fluid (represented by m and n) in the solving domain can be expressed as follows.

Continuous equation:

$$\frac{\partial}{\partial \tau}\left(\alpha_m \rho_m\right)+\nabla \cdot\left(\alpha_m \rho_m \vec{U}_m\right)=\dot{m}_{mn}-\dot{m}_{nm} \tag{1}$$

Momentum equation:

$$\frac{\partial}{\partial \tau}\left(\alpha_m \rho_m \vec{U}_m\right)+\nabla \cdot\left(\alpha_m\left(\rho_m \vec{U}_m \vec{U}_m-\mu_m^*\left(\nabla \vec{U}_m+\left(\nabla \vec{U}_m\right)^T\right)\right)\right)=\alpha_m\left(\rho_m g-\nabla p_m\right)$$
$$+\vec{F}_{mn}+\dot{m}_{mn}\vec{U}_m-\dot{m}_{nm}\vec{U}_n \tag{2}$$

Energy equation:

$$\frac{\partial}{\partial \tau}\left(\alpha_m \rho_m i_m\right)+\nabla \cdot\left(\alpha_m\left(\rho_m \vec{U}_m i_m-\lambda_m^* \nabla T_m\right)\right)=q_{mn}+\dot{m}_{mn} i_m-\dot{m}_{nm} i_n \tag{3}$$

2.2. Closure Relations

In order to determine the flow characteristics and distribution of two-phase fluid accurately, the Realizable k-ε turbulence model is adopted for the liquid phase and the vapor phase. More details of the Realizable k-ε turbulence model can be found in Ref [6].

2.2.1. Wall boiling model

According to RPI wall boiling model proposed by Kurul and Podowski , the total heat flux from heated wall to the fluid is partitioned into three components, the single-phase convective heat flux q_C, the evaporate heat flux qE and the wall quenching heat flux q_Q.

ISSN: 2472-3703 DOI: 10.6911/WSRJ.202007_6(7).0038

$$q_W = q_C + q_E + q_Q \tag{4}$$

These three heat fluxes can be expressed as,

$$q_C = h_C(T_w - T_b)(1 - A_b) \tag{5}$$

$$q_E = V_d N_w \rho_v r f \tag{6}$$

$$q_Q = \frac{2\sqrt{\lambda_l \rho_l c_{p,l} f}}{\sqrt{\pi}}(T_w - T_l) \tag{7}$$

Where h_C denotes the single phase turbulent heat transfer coefficient; T_w and T_b are the wall and fluid temperature, respectively; ρl and ρ_v are the density of liquid and vapor phase, respectively; r is the latent heat of evaporation; V_d is the volume of the bubbles based on the bubble departure diameter; $c_{p,l}$ and λ_l are the specific heat and conductivity of liquid phase, respectively. Ab is the proportion of heated wall covered by nucleating bubbles, estimated by:

$$A_b = \min\left(1, K\frac{N_w \pi d_{bw}^2}{4}\right) \tag{8}$$

Where d_{bw} is the bubble departure diameter, given by Tolubinsky model:

$$d_{bw} = \min\left(0.0006 \cdot e^{\left(-\frac{\Delta T_{sub}}{45.0}\right)}, 0.0014\right) \tag{9}$$

And K is an empirical constant estimated by Del Valle and Kenning equation:

$$K = 4.8\exp\left(-\frac{\rho_l c_{p,l}(T_w - T_l)}{80\rho_v r}\right) \tag{10}$$

And N_w is the active nucleate site density, given by Lemmert and Chawla model:

$$N_w = 210^{1.805}(T_w - T_{sat})^{1.805} \tag{11}$$

Where T_{sat} is the saturated temperature. f is the frequency of bubble departure, given by Cole correlation :

$$f = \frac{1}{T} = \sqrt{\frac{4g(\rho_l - \rho_g)}{3d_{bw}\rho_l}} \tag{12}$$

Where g is the gravitational acceleration.

2.2.2. Interphase mass, momentum, energy transfer

ISSN: 2472-3703 DOI: 10.6911/WSRJ.202007_6(7).0038

The heat transfer per unit volume in a vertical tube can be considered as the result of mutual movement of the two-phase fluid, which can be expressed as:

$$Q_{lv} = h_l A_{lv}\left(T_{sat} - T_l\right) \tag{13}$$

$$Q_{vl} = h_v A_{vl}\left(T_{sat} - T_v\right) \tag{14}$$

Where $A_{lv}=A_{vl}=6\alpha_v/D_b$ represents the interfacial area concentration. The mean bubble diameter in the bulk flow, D_b, can be given by Ünal:

$$Db=\begin{cases} 0.0015 & \Delta T_{sub}<0 \\ 0.0015-0.0001\Delta T_{sub} & 0\le\Delta T_{sub}<13.5 \\ 0.00015 & \Delta T_{sub}\ge 13.5 \end{cases} \tag{15}$$

Where $\Delta T_{sub}=T_{sat}-T_b$ represents the local subcooling.

The heat transfer coefficient across the interface of the liquid phase (hl) can be obtained by Hughmark model:

$$Nu=\begin{cases} 2+0.6Re^{0.5}Pr^{0.33} & 0\le Re<776.06,\ 0\le Pr<250 \\ 2+0.27Re^{0.62}Pr^{0.33} & Re\ge 776.06,\ 0\le Pr<250 \end{cases} \tag{16}$$

And the heat transfer on the vapor side of the interface can be simulated by zero resistance model, that is $T_{sat}=T_v$.

The mass exchange between the phases can be considered a vaporization process:

$$m_{lv} = \frac{Q_{lv} + Q_{vl}}{r} \tag{17}$$

The momentum exchange in the interphase is mainly caused by the interfacial forces, which are composed of buoyancy, virtual mass force, turbulent dissipation force, and drag force. Buoyancy is calculated by Moraga model; Virtual mass force is calculated by Drew and Lahey; Turbulent dissipation force is calculated by Burns model; Drag force is calculated by Ishii model.

2.3. Physical Model and Boundary Conditions

A 3D physical model is established to model a 1.56m long vertical tube with an inner diameter D of 6.0mm. To ensure the accuracy of the flow in the phase change region, the inlet and outlet of the tube are increased to 5D length extension. The length of heated section is 1.5m. The mass flux rate inlet is used as the inlet boundary, and fully developed velocity profiles and accompanying turbulent properties are employed in the inlet. The pressure outlet is used as the outlet boundary and the secondary thermal boundary conditions are used for the wall. A no slip

ISSN: 2472-3703 DOI: 10.6911/WSRJ.202007_6(7).0038

boundary is adopted in both the vapor and liquid phases. Properties of R290 used in simulations are saturated values calculated at the outlet pressure.

3. MESH INDEPENDENT SOLUTION AND MODEL VALIDATION

In order to get an accurate computation of a solution, a standard hexahedral mesh is used to divide the solution domain, with fine meshes near the wall to ensure that y+ value satisfies the requirements of the used turbulence model and wall function, as shown in Fig 1. The simulations are performed with four different meshes as shown in Table 1. The results become mesh-independent when the mesh amount reaches 402809 elements. Therefore, the mesh number (402809 elements) is used in the present study. The mesh is generated by ANSYS ICEM CFD.

The governing equations and diffusion terms are discretized by the finite volume method and central difference scheme, respectively. The volume fraction term is discretized by QUICK method, while the other convection terms are treated applying second-order upwind method. The coupling between pressure and velocity performed with Coupled Implicit Solver is used. When relative residuals of the control volumes in the governing equations are smaller than 10^{-4}, the results are converged.

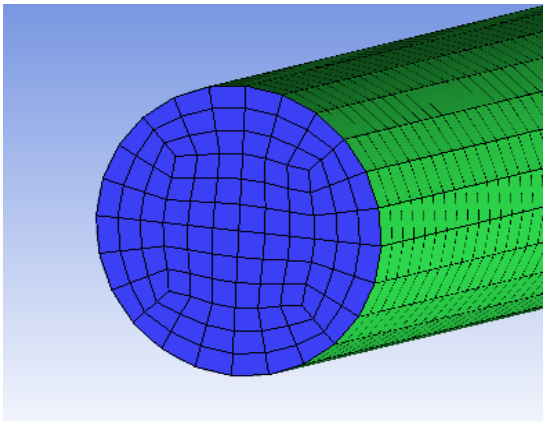

Figure 1. Grid model

In order to verify the correctness of the model, the simulation result is compared with the subcooled nucleate flow boiling relationship of Liu and Winterton. More details of the correlation can be found in Ref [18]. The results are shown in Fig 2, where xth denotes thermodynamic equilibrium quality. It can be seen from the figure that the relative error between most numerical results and correlation is within 20%, which satisfies the calculation accuracy requirement. The location of ONB is ensured by identifying the point where the heat transfer coefficient increases rapidly.

ISSN: 2472-3703 DOI: 10.6911/WSRJ.202007_6(7).0038

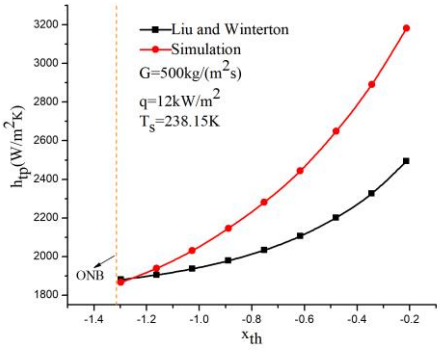

Figure 2. Comparison between simulation and correlation

Table 1. Mesh independent validation

Mesh number	Outlet void	Absolute deviation	Error percentage
201465	0.24690	-	-
302137	0.24733	0.00043	0.174%
402809	0.24757	0.00024	0.097%
503481	0.24772	0.00015	0.061%

4. RESULTS AND DISCUSSION

For this section, the operation condition of the simulation is as follows: G=500kg/m²s, q=12kW/m², T_s=238.15K, ΔT_{sub}=10. This section analyses the characteristics of two-phase heat transfer and flow of R290 during subcooled flow boiling from different aspects, including vapor volume fraction, wall and bulk temperature, vapor and liquid velocity and heat transfer coefficient. Two directions are used for convenience, named axial direction(y) and radial direction(x), respectively.

4.1. Axial and radial vapor volume fraction

Fig 3(a) and (b) shows the axial and radial profiles of α, respectively. The amount of vapour begins to increase after ONB. However, the amount of void remains low and fairly constant. At a certain location, the slope of the void growth curve changes significantly resulting in a dramatic increase in the amount of vapor.

As can be seen from Fig 3(b), radial void increases rapidly first and diminishes towards the channel core, resulting in a peak void near the wall. There is a slow trend of void decrease in the core along the axial direction. The reason for this phenomenon is that bubbles are generated near the heated wall and form a bubble boundary layer. After detaching from the wall, bubbles condensate in the subcooled liquid core. With the gradual warming of core liquid, the effect of condensation is weaken.

ISSN: 2472-3703 DOI: 10.6911/WSRJ.202007_6(7).0038

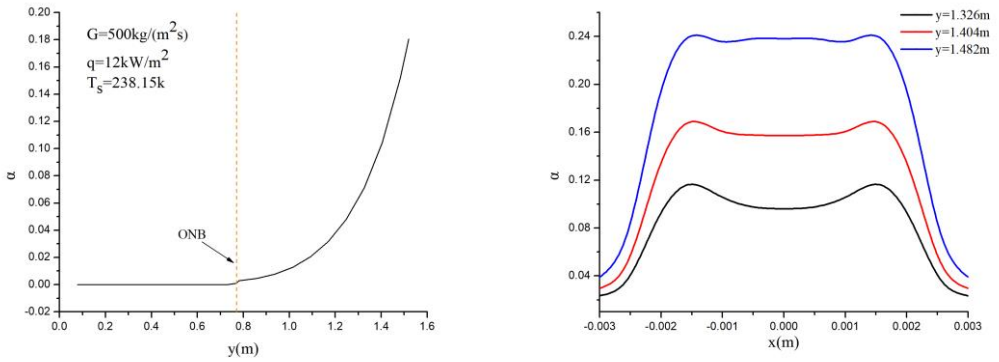

Figure 3. The variation of vapor volume fraction along (a) axial and (b) radial direction

4.2. Axial Wall Temperature and Bulk Temperature

Fig 4. shows the axial wall temperature T_w and bulk temperature T_b profiles. In the entrance region, the temperatures of wall and bulk rise at a constant rate, which can be interpreted by the weak heat transfer effect. When the wall temperature exceeds the liquid saturation temperature up to a certain superheat, nuclear boiling takes place and the heat transfer is enhanced. As a result, the wall temperature experiences a sharp drop and then rises again at a relatively low rate. The difference between wall temperature and bulk temperature decreases gradually in the subcooled region. The bulk temperature reaches the saturation temperature finally.

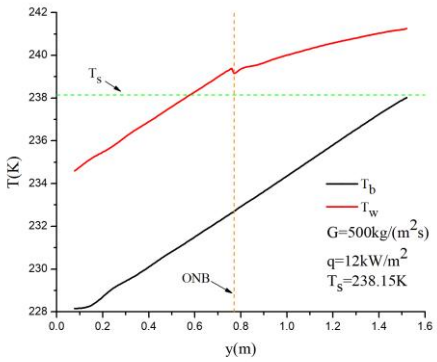

Figure 4. Axial wall and bulk temperature

4.3. Axial Vapor and Liquid Velocity

Fig 5. and Fig 6. present the axial vapor and liquid velocity and the slip ratio (defined as vapor-to-liquid velocity ratio) profiles. The liquid velocity keeps nearly unchanged in the single phase liquid convection region because the fluid density remains constant. In the subcooled flow boiling region, void increases and the average density of fluid is reduced along the channel. Hence, the vapor and liquid velocity increase generally while the vapor velocity rises more quickly. During the initial period of nuclear boiling, bubbles cover the wall and suffer from a large drag force. Therefore, the vapor velocity is smaller than the liquid velocity initially and the slip ratio is less than 1. As the bubbles grow and detach from the wall, lift force has a great effect on bubbles. Due to the difference in vapor and liquid density, the vapor velocity is greater than the liquid velocity finally. Meanwhile, the slip ratio exceed 1 gradually and approaches 1.047 near the outlet.

ISSN: 2472-3703 DOI: 10.6911/WSRJ.202007_6(7).0038

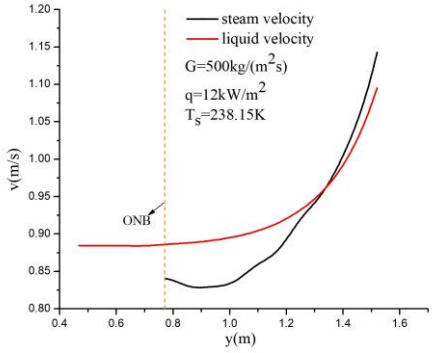

Figure 5. Axial steam and liquid velocity

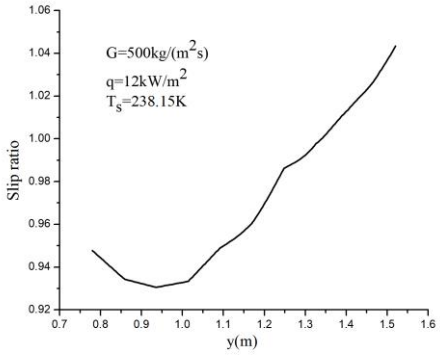

Figure 6. Axial slip ratio

4.4. Axial Heat Transfer Coefficient

Fig 7. shows the axial heat transfer coefficient profiles. The heat transfer coefficient declines at the beginning of single phase connective heat transfer region because of the development of thermal boundary layer. Then the heat transfer coefficient changes little because the temperature difference between wall and bulk temperature remains constant. There is an obviously increase of the heat transfer coefficient at the location of ONB. In subcooled nuclear boiling region, the heat transfer continues to be enhanced due to turbulent effects stemming from high mixing caused by motion of bubbles and axial fluid acceleration. Hence, the two phase heat transfer coefficient rises rapidly and is 1.8 times as large as the single phase heat transfer coefficient near the outlet.

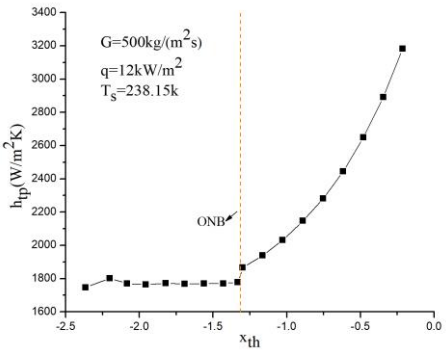

Figure 7. Axial heat transfer coefficient

ISSN: 2472-3703 DOI: 10.6911/WSRJ.202007_6(7).0038

5. CONCLUSIONS

This study numerically investigated the two-phase heat transfer and flow of R290 during subcooled flow boiling in a vertical tube at low saturation temperature under a low mass flux and heat flux operation condition. The 3D simulations were carried out using two-fluid model and RPI wall boiling model on the platform of Fluent. The numerical results were verified to be accurate comparing with an experimental correlation. Worthy findings from the present study are as follows:

(1)Radial void increases rapidly first and diminishes towards the channel core, resulting in a peak void near the wall. The trend of void drop becomes slow in the core along the axial direction.

(2)The wall temperature drops sharply at ONB and then rises at a relatively low rate. In the subcooled flow boiling region, the difference between the wall and bulk temperature decreases gradually.

(3)The vapor velocity is lower than the liquid velocity at the beginning of subcooled flow boiling. With the increase of the void, the vapor velocity accelerates more quickly than the liquid velocity. The slip ratio is up to 1.407 near the outlet.

(4)The heat transfer coefficient waves little in the single phase region, while it increases rapidly in the two-phase region which is 1.8 times larger than that in single phase region near the outlet region.

REFERENCES

[1] S.M. Peyghambarzadeh, A. Vatani, M. Jamialahmadi: Application of asymptotic model for the prediction of fouling rate of calcium sulfate under subcooled flow boiling, Applied Thermal Engineering, Vol. 39(2012), 105-113.

[2] K. Choi, A.S. Pamitrana, J. Ohb, et al. Pressure drop and heat transfer during two-phase flow vaporization of propane in horizontal smooth minichannels, International Journal of Refrigeration, Vol. 32(2009), 837-845.

[3] G. Lillo, R. Mastrullo, A.W. Mauro, et al. Flow boiling heat transfer, dry-out vapor quality and pressure drop of propane (R290): Experiments and assessment of predictive methods, International Journal of Heat and Mass Transfer, Vol. 126(2018), 1236-1252.

[4] E.F. Chen, Y.Z. Li, X.H. Cheng: CFD simulation of upward subcooled boiling flow of refrigerant-113 using the two-fluid model, Applied Thermal Engineering, Vol. 29(2009), 2508-2517.

[5] Y.P. Gao, S.Q. Shao, H.B. Xu, et al. Numerical investigation on onset of significant void during water subcooled flow boiling, Applied Thermal Engineering, Vol. 105(2016), 8-17.

[6] T.H. Shih, W.W. Liou, A. Shabbir, et al. A new k-epsilon eddy viscosity for high Reynolds number turbulent flows, Comput. Fluids, Vol. 24 (1995), 227–238.

[7] N. Kurul, M. Podowski: On the modeling of multidimensional effects in boiling channels, ANS Proc. 27th National Heat Transfer Conference(Minneapolis, USA, 1991), Vol.1, p.28.

[8] E. Krepper, B. Koncar, Y. Egorov: CFD modeling of subcooled boiling-concept, validation and application to fuel assembly design, Nuclear Engineering and Design, Vol. 237(2007), 716–731.

[9] D. Valle, D.B. Kenning: Subcooled flow boiling at high heat flux, Int. J. Heat Mass Transf, Vol. 28(1985), 1907–1920.

[10] M. Lemmert, J.M. Chawla: Influence of flow velocity on surface boiling heat transfer coefficient, Heat Transfer Boil, Vol. 237 (1977) 247.

ISSN: 2472-3703 DOI: 10.6911/WSRJ.202007_6(7).0038

[11] R. Cole: A photographic study of pool boiling in the region of the critical heat flux, AIChE J, Vol. 6 (1960), 533–538.

[12] Ünal: 1976. Maximum bubble diameter, maximum bubble-growth time and bubble growth rate during the subcooled nucleate flow boiling of water up to 17.7 MN/m2, Int. J. Heat Mass Transfer, Vol. 19 (1976), 643–649.

[13] J.L. Xu, T.N. Wong, X.Y. Huang, X.Y: Two-fluid modeling for low-pressure subcooled flow boiling, Int. J. Heat Mass Transfer, Vol. 49 (2006), 377–386.

[14] F.J. Moraga, F.J. Bonetto, R.T. Lahey: Lateral forces on spheres in turbulent uniform shear flow, Int. J. Multiph. Flow, Vol. 25(1999), 1321–1372.

[15] Drew, Lahey: In particulate two-phase flow(Butterworth-Heinemann, USA, 1993), p.509.

[16] A.D. Burns, T. Frank, I. Hamill, et al. The Favre averaged drag model for turbulent dispersion in Eulerian multi-phase flows, Proceedings of the 5th International Conference on Multiphase Flow, ICMF, Vol. 4(2004).

[17] M. Ishii, N. Zuber: Drag coefficient and relative velocity in bubbly, droplet or particulate flows, AIChE J, Vol. 25(1979), 843–855.

[18] Z. Liu, R.H.S. Winterton: A general correlation for saturated and subcooled flow boiling in tubes and annuli, based on a nucleate pool boiling equation, Int. J. Heat Mass Transf, Vol. 34 (1991), 2759–2766.